

Climate as main factor controlling the sequence development of two Pleistocene alluvial fans in the Vienna Basin (eastern Austria) – A numerical modelling approach

Bernhard C. Salcher^{a,c,*}, Robert Faber^b, Michael Wagreich^c

^a Department of Earth Sciences, ETH-Zurich, Sonneggstrasse 5, CH-8092 Zurich, Switzerland

^b TerraMath Geoscientific Software, Hauptstrasse 59, A-3021 Pressbaum, Austria

^c Department of Geodynamics and Sedimentology, University of Vienna, Althanstrasse 14, A-1090 Vienna, Austria

ARTICLE INFO

Article history:

Accepted 16 June 2009

Available online 17 July 2009

Keywords:

Alluvial fan
Climate
Pleistocene
Subsidence
Numerical modelling

ABSTRACT

Tectonics, climate, base level and source lithology are the main controlling factors on alluvial fan development and evolution. In this study a numerical model approach was used to investigate climate-induced aggradation and degradation cycles, the influence of tectonic subsidence, and the impact of an axial main river on Austria's largest Pleistocene alluvial fan setting, the Mitterndorf Basin, eastern Austria. A simulation time frame of 25 ka was applied. Climatic variations were mainly modelled through variations in sediment supply, whereas the impact of subsidence was modelled through variations in slip rates along faults. Incision and aggradation tendencies of the axial main river were modelled by rising or lowering of the water level. The sequence development and geometry of Mitterndorf Basin's alluvial fans are mainly controlled by Pleistocene climate oscillations. Cold periods generally led to a decrease in vegetation cover and to an increase of periglacial weathering processes which is associated with abundant sediment release and aggradation on fan surface. In contrast, decreasing sediment supply and increasing precipitation during warmer periods led to fan degradation. Our models indicate that the alluvial fan development is primarily affected by the distinct sediment supply pulses during phases of short climatic perturbations. Subsidence becomes the determining factor again when models approach a steady-state behaviour. Similarly, the impact of the axial main river becomes more important during simulated warm periods when sediment release to the drainage basin is low. The overall basin slope additionally controls the evolution of fan and drainage. Variations in sediment supply and subsidence do also significantly control the long term evolution of the drainage network during simulated warm periods and thus control the sequence preservation potential of fans and therefore its long term sequence evolution.

© 2009 Elsevier B.V. All rights reserved.

1. Introduction

Tectonic, climate and base-level related factors are generally assumed to act as main influencing factors on alluvial fan development (Bull, 1977).

Climatically induced sediment supply is supposed to be the primary control (e.g. Harvey et al., 1999; Harvey, 2002a,b). Especially during the Pleistocene, distinct oscillations have a large influence on the sediment supply to discharge ratio (e.g. Van Husen, 2000; Vandenberghe, 2002; Bogaart et al., 2003; Vandenberghe, 2008). The discharge-to-sediment supply ratio influences whether fans undergo aggradation or degradation (Wells and Harvey, 1987). Similarly, if fans toe out on unstable base levels, response may cause incision or fan aggradation. The significant impact of Quaternary glacial–interglacial cycles on alluvial sequence development at a basin-scale has been described e.g. by Shanley and McCabe (1994) and Weissmann et al. (2002, 2005). A depositional model

for Austria's largest Pleistocene basin over the time span between MIS 3 and MIS 1 has been presented by Salcher and Wagreich (in press). Interactions of all controlling factors are complex. To better understand these interactions we chose a numerical model approach to simulate the landscape evolution during the last glacial/interglacial cycle.

Multi-process landscape models which consider two or more mutually interacting geomorphic processes have found a widespread application covering processes like fluvial transport of sediment, weathering or landsliding (e.g. Willgoose et al., 1991; Slingerland et al., 1994; Tucker and Slingerland, 1994; Braun and Sambridge, 1997). Similar, studies on numerical forward models dealing primarily with stratigraphic sequence evolution are numerous (cf. Paola, 2000). Recent studies have been presented by e.g. Warrlich et al. (2008), Waltham et al. (2008) and Braun et al. (2008). Numerical simulations which are focused on the morphologic or sedimentologic evolution of alluvial fans were carried out e.g. by De Chant et al. (1999) and Allen and Densmore (2000), respectively.

A series of numerical models simulated the impact of changing sediment supply, subsidence and base-level change on two stream dominated mountain-front fans in the study area. Strong variations

* Corresponding author.

E-mail address: bernhard.salcher@erdw.ethz.ch (B.C. Salcher).

in sediment supply modelled the relevance of strong climatic fluctuations in the hinterland corresponding to glacials, interglacials or interstadials (cf. Fink and Kukla, 1977; Willis et al., 2000; Van Husen, 2000). Numerical experiments cover a time frame of 25 ka affecting the last cold/warm transition from MIS 2 to MIS 1 in Austria's largest Pleistocene Basin. The principle knowledge on the regional climate and basin evolution (Salcher, 2008; Salcher and Wagreich, in press) was used to calibrate a reference model from which alterations in sediment supply, subsidence and elevation change of the axial main river were observed.

Decrease in vegetation density and increase in weathering were modelled through an increase of sediment release to the basin (cf. Bull, 1991, 1996; Leeder et al., 1998). Warmer periods are associated with increased precipitation, reduced weathering and a higher vegetation density around the study area (Fink and Kukla, 1977; Van Husen, 2000). This scenario was simulated through a linear reduction in sediment supply leading to higher discharge-to-sediment supply ratios and associated stream incision and fan abandonment. Resulting Models were evaluated and compared with the real world.

2. Regional settings

The rhomb-shaped, SW–NE trending Miocene Vienna Basin extends about 200 km from the Eastern Alps into the West Carpathians. Active deformation is related to several Pleistocene sub-basins (Fink, 1955) along the Vienna Basin Transfer fault. The largest of these Pleistocene sub-basins is the Mitterndorf Basin (Fig. 1) with an area of approximately 270 km². It is supposed to be a strike-slip duplex (Decker et al., 2005) which has evolved since the middle Middle Pleistocene (Salcher, 2008). The basin has a maximum width of not more than 15 km, a length of about 60 km (Fig. 1) and reaches maximum sediment thicknesses of 170 m. Two mountain-front alluvial fans fill the South of the Mitterndorf Basin with up to 110 m of massive gravels. Both fans are stream dominated and comprise mainly massive, coarse grained fluvial gravels and cobbles. Gravels and cobbles are related to aggradational responses associated with Pleistocene cold periods (Küpper, 1950). Coarse grained

series are interrupted by paleosols which are indicating periods of undisturbed soil development on fan surfaces. The youngest aggradational event on both fans can be constraint to the MIS 2 cold period (Salcher and Wagreich, in press). Times around the last glacial maximum are related to a periglacial climate associated with a low vegetation density, strong weathering (conglifraction) and low precipitation values. Large quantities of debris (Fink and Kukla, 1977; Van Husen, 2000) were released due to the absence of vegetation and glaciation in the alpine hinterland during that time. In contrast warmer periods are associated with increased precipitation, reduced weathering and a higher vegetation density around the study area (Van Husen, 2000). Aggradation on both fans ended at around c. 12 ka (Salcher and Wagreich, in press). No active deposition has occurred on both either fan since that time, forcing soil formation processes on their abandoned surfaces. The northern fan (Piesting River alluvial fan – Piesting fan) is 88 km² in size, the adjacent Schwarza River alluvial fan (Schwarza fan) is about 120 km² (Fig. 1). The catchment area of the Piesting fan covers approx. 280 km², with its highest elevation 1723 m above sea level. The elevation of the fan apex is 310 m above sea level. The catchment area of the Schwarza fan covers about 670 km², with a highest elevation of 2076 m above sea level. The elevation of the fan apex is about 370 m above sea level. Weak glaciation (several sq km) of highest points during Pleniglacial is evident in the Schwarza drainage basin (Van Husen, 1987).

3. Materials and methods

3.1. Modeling software (WinGeol/SedTec) and data preparation

WinGeol/SedTec is a finite difference code based on WinGeol (TerraMath software). The software was firstly presented at the European ENTEC (Environmental Tectonics) spring workshop 2002, (University of Vienna; cf. Faber and Wagreich, 2005). There is no connection to the SedTec Modeling Group (Royal Holloway University, UK) nor the software SedTec2000 (Boylan et al., 2002).

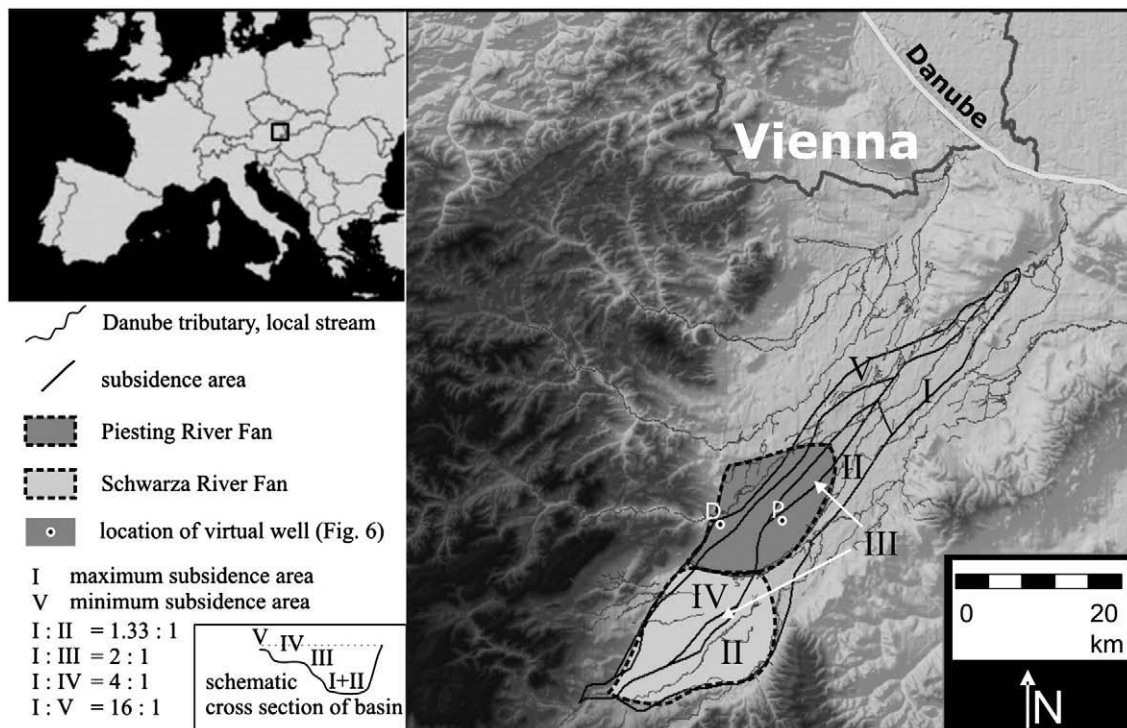


Fig. 1. Shaded DEM of the southern Vienna Basin. The Mitterndorf basin area is shown by the outline of the subsidence map created based on log, seismic and gravity data. P- (proximal) and D- (distal) points mark the location of the virtual well logs (Fig. 6).

The multi-process landscape and stratigraphic forward modelling software WinGeol/SedTec (version 1.2×) simulates erosion, transport and deposition processes. Temporal changes of environmental conditions are supported using time tables, which store changes of sediment supply, precipitation, base level and vertical tectonic displacement. The modelled stratigraphic record is saved at the end of each time step.

In WinGeol/SedTec a strict separation of data structures / associated methods and modelling functions/methods is given to shorten debugging times and the readability of the code. The software support 3D visualizing of all model results together with a wide range of (geological) data like e.g. grid, vector and well data (tables).

3.2. Definitions

A short definition of frequently-used terms.

3.2.1. Calculating cycle

Each time step consists of numerous calculation cycles. During a calculating cycle all cells of a model are processed at least once. A calculation step defines the smallest temporal unit of a simulation.

3.2.2. Time step

A time step represents a number of calculation cycles after which the actual state of the simulation is saved. In this study all time steps have identical durations (3125 years). After the end of a time step new sediments are stored within a new grid layer.

3.2.3. Process sequence order

Defines the sequence in which the single cells of the model are processed (for explanations see [Section 3.4.2](#)).

3.3. Data structure

WinGeol/SedTec models are derived from grid data are therefore based on equal spaced cells in x and y directions whereas the z dimension is variable. The smallest unit of a model is called a cell. A cell itself is defined as a volume with no internal structure. The number of cells is given by the number of rows and columns and multiplied with the number of time steps. A further layer is used as temporary storage for not yet deposited material. Every cell stores a number of variables which are divided into two groups:

- Condition: state variables like local flow, vertical tectonic offset, cumulative erosion and deposition.
- Material content (grouped by material and grain size (if a grain size reduction algorithm is used), water is stored as solid or fluid).

All values are stored internally as 4 byte floating point values.

This structure was chosen because of its simplicity, good performance and format of used input data.

Important consequences of the data structure for the simulation are:

- Each cell has 8 neighbours on the topographic surface of the grid and therefore just 8 possible directions where a material flow can be directed to.
- A fixed minimum resolution in x and y directions — transport distances are always a multiple of a cell size.
- Tectonics are limited to vertical displacement as cells are fixed to their x and y position.

3.4. Data structure related methods

3.4.1. Model administration

Low level functions represent the basic management (e.g. model initialization). Medium level functions retrieve or set values which

describe the relationship between two or more cells (e.g. calculation of difference matrices, finding the lowest neighbouring cell, retrieving the status of a neighbour). Functions which affect more cells than the direct neighbours (like the transport path) are high level functions. Functions do not decide if / where and how much is eroded / moved or deposited — this is the task of the algorithms ([Section 3.5](#)).

3.4.2. Process sequence calculation and support for velocity modelling (out of order processing)

Processes in nature occur more or less parallel with or without dependency on each other. As long as processes do not interact (spatial or temporal separation) there is no conflict within the simulation. This can be guaranteed if transport per calculation step is limited to the directly neighbouring cells. Every cell is eroded one time per cycle and is allowed to move a certain mass to one or more directly neighbouring cells. Even if the erosion/transport function used returns different mass volumes to be transported (based on variation of the transport coefficient), the speed of transport itself stays constant. To model different transport velocities, a target cell (a grid cell which receives material from a source cell) is turned into a source cell itself after receiving material (within one calculation step, we call this “out of order processing”). Hence some cells might be processed several times during a calculation step. To avoid errors within the mass balance there are 2 possibilities:

- The arriving mass is not interacting with the new source cell (only some cell properties — like elevation — will be used to calculate how much material will go further)
- Interaction is allowed, the newly arrived material can mix with material which is already present (material properties are changed by mixing).

As a consequence of b, the transport process will be guided by the properties of the mixed material, and some material originated in the target cell will be transported to the next target cell. Later in the same calculation step the target cells themselves will become the primary source cells. In the case where the calculation starts with the original status at the beginning of the calculation step, some material which was already transported to another location might be processed again and therefore conservation of mass principle is violated. Hence, the algorithm has to proceed with the update status. In a typical grid based data set, the calculation will start at the cell with the index 0 and stop at the last cell at the opposite corner. This simple cell after cell operation (in the sequence they are stored in the computer memory) will have a huge influence on the result as only later processed cells may have received material from other cells already. The process used, sequence sorting, determines which cells are more likely to be processed earlier than others. WinGeol/SedTec offers different sorting options to study and (sorting by elevation, slope or random sequence). Simulations in this study used a sorting by the topographic elevation algorithm.

During the “out of order” process the full sequence of erosion, transport and deposition is executed and repeated until a certain amount of time is consumed, the speed drops below a minimum value (no transport) or a model boundary is reached.

As transport distances (depending on the situation) are increased, the number of calculation cycles is considerably smaller than within models that only support transport to the direct neighbouring cells. Rather inactive cells are not processed as often as active cells (more often accessed from other cells, higher flow rate). In our study, the number of calculation cycles is in the range of 40 to 400, whereby 400 was only used to check the stability of the results. Stability in this case means, that the results using 40 calculation steps did not differ too much (max. 15%) from the results achieved with 400 calculation steps.

If “out of order” processing is used, 40 is just the very minimum number. Cells located in the e.g. channels are processed many more times (several 10,000 times). As the “out of order” processing

algorithm does not waste processing time on inactive cells, the calculation speed is normally much increased.

The routing algorithm used in WinGeol/SedTec is principally non distributary, as only one target cell (of the directly neighbouring cells) is supported during a single transport operation. Distributary channel networks develop within a calculation cycle because “out of order processing” allows multiple transport operations within one calculation step on one cell and results are therefore comparable to a routing algorithm which directly supports distributaries.

Direct support to access several target cells at one time is not implemented as this would lead to a geometrical growth of calculation time with transport distance (in our case approximately by the factor 4^n , n = transport distance divided by cell size).

3.4.3. Related modelling functions and features

3.4.3.1. Determining the transport target. Transport direction is determined by (a) the evaluation of the neighbourhood matrix and (b) by adding a movement vector from prior calculation cycles (v_0 , if present).

The software calculates the direction of the gravity vector v_1 , which is situated between the lowest cell and its lower neighbour. The final transport direction is determined by addition of v_0 and v_1 . The transport distance is calculated by algorithms introduced in 3.3.3. (Transport distance and velocity).

3.4.3.2. No-data areas and model boundaries. No-data areas and model boundaries are treated in the same way. In both cases no information about elevation and material is available. WinGeol/SedTec estimates the local slope at the no-data area by extrapolation of the local slope to avoid unrealistic effects like incision or damming at the model boundary.

3.4.3.3. Time dependent environmental changes. WinGeol/SedTec supports time dependent alteration of environmental conditions like sediment supply, precipitation and tectonic (vertical) movement and base-level fluctuations. The values are read from ASCII tables (a separate one for tectonic processes) and are interpolated linearly.

3.5. Algorithms

3.5.1. Regolith production

In nature regolith production is mainly controlled by climate-related factors like e.g. weathering rates. The production rate decays exponentially with increasing regolith thickness. According to Anderson and Humphrey (1990) the following formula was used:

$$E_w = k_w e^{(-R/R_0)} \quad (1)$$

E_w	rate of descent [m/a]
k_w	original bedrock weathering rate (at surface) [m/a]
R_0	thickness of regolith where weathering rate is equal to $1/e k_w$ [m]
R	regolith thickness [m]
e	Euler's number (2.71828...) [–]

Weathering rates for different (bed-)rock types are used according to Allen and Allen (2005).

3.5.2. Erosion and transport

WinGeol/SedTec models erosion using two different approaches. Hillslope erosion is implemented using the diffusion equation. Fluvial incision is processed by using the stream-power based approach.

3.5.2.1. Diffusion. Field observations show that erosion is proportional to the local slope (Culling, 1960; Andrews and Bucknam, 1987). To describe this observation we used a diffusion equation (Allen and Allen, 2005):

$$\delta q / \delta x = -\rho_b \delta z / \delta t \quad (2)$$

$$q = -k \delta z / \delta x \quad (3)$$

q	mass flow (discharge of mass per unit width) [kg/m]
ρ_b	bulk density of moved regolith [kg/m ³]
k	transport coefficient, diffusion rate [–]
δz	elevation difference [m]
δx	horizontal distance [m]
δt	time interval [s]

Combining Eqs. (2) and (3) mass diffusion can be written as:

$$\delta z / \delta t = \kappa \delta^2 z / \delta^2 x [\text{m/s}] \quad (4)$$

$$\kappa = k / \rho_b \left[1 / (\text{kg/m}^3) \right] \quad (5)$$

κ diffusivity

Material recently deposited (e.g. during the last time step) is handled with a higher transport coefficient (6, $k_{\text{unconsolidated}}$).

The transport coefficient is material dependent for bedrock. For material in transport, it is calculated by approximation of the volume ratio of fluid to solid components. The usage of a bedrock transport coefficient is not appropriate as the bedrock transport coefficients describe solid rocks. The transport coefficient of water is set to 1 (assumed to behave like a Newtonian liquid without viscosity). The transport coefficient for dry unconsolidated clastic material is a user-defined setting, which is set between the transport coefficient of water and the transport coefficients of bedrock material. The value used for $k_{\text{unconsolidated}}$ within this study was calibrated to 0.2 which was found to best-fit by running a series of sub-area models.

$$k_{\text{transp}} = k_{\text{unconsolidated}} (V_{\text{sol}} / (V_{\text{sol}} + V_{\text{fl}}) + k_{\text{fluid}} (V_{\text{fl}} / (V_{\text{sol}} + V_{\text{fl}})) \quad (6)$$

V_{fl}	volume of fluid (water) [m ³]
V_{sol}	volume of unconsolidated, solid material [m ³]
$k_{\text{unconsolidated}}$	transport coefficient of dry unconsolidated sediment (user-defined setting) [–]
k_{fluid}	transport coefficient of water [–]
k_{transp}	transport coefficient of new sediment on the source cell [–]

Denudation rates for the Piesting and Schwarza catchment area range around c. 200 mm/ka between c. 30 and 10 ka B.P. (using the mass balance equation of Einsele and Hinderer, 1998). The average slope in the catchment is c. 10°, which gives an average elevation difference from one to another cell of 17.6 m (assuming a cell size of 100 m). A transport coefficient set to 10^{-2} would lead to an average surface erosion of 176 mm/ka. The coefficient of 10^{-2} was found independently from the denudation calculation by comparing simulated sequence thicknesses with outcrop and well-log data. Because of the homogenous properties of the bedrock within the study area, we decided to use a constant k of 10^{-2} .

3.5.2.2. Bedrock incision. For calculating the incision of streams an approach based on the widely understood stream-power law approach was chosen (the stream-power law is for example discussed in Allen and Allen, 2005), incision is therefore a constraint of material, discharge and local slope.

$$\delta z / \delta t = -c_b Q^m (dz/dx)^n \tag{7}$$

c_b bedrock incision coefficient [–]
 Q discharge [m³/s]
 m, n empirical coefficients [–]

Published values for m and n are in the range of 0.2 to 0.4 (Stock and Montgomery, 1999). For c_b , values are in the range of 10^{–2} (mud) to 10^{–7} (granite) mm/a.

We calibrated a value of 1 for n and m . This difference from published data has two main reasons:

During the simulation the bedrock is recurrently covered with sediment which has to be removed. Therefore not the “full” energy of the discharge is available for bedrock incision:

- Over 2/3 of the material moved is reworked sediment (in whole simulation area).
- In river channels which are in equilibrium, bedrock incision is very low and even in incising rivers the bedrock to reworked sediment ratio is rarely larger than 1%.

For these reasons the exponent m in our simulations must be considerably higher than given by Stock and Montgomery (1999).

Values for c_b are based on k (transport coefficient) for bedrock material, for unconsolidated material on $k_{unconsolidated}$ and for material in the state of transport by a linear interpolation based on the water content (Eq. (6)).

3.5.2.3. Transport distance and velocity. In Section 3.4.2 “out of order” processing was introduced which gives the possibility of moving material further than just to the next neighbouring cells within one calculation step. To estimate how far the transport will go, the transport velocity is necessary; we assume that transport speed depends on:

- Gravitation, slope and processes of friction: the friction of the moving mass at the surface and the friction between its particles
- and solid to fluid ratio, as water content has a huge influence on viscosity and therefore on the speed of mass flows.

Exact parameters for friction are nearly impossible to estimate from the input data of the model, therefore the parameters were optimized using data from the literature. A direct usage of formulae used for stream velocity calculation is not possible as parameters like depth of stream or width are not available.

3.5.2.4. Integration of the fluid/solid volume ratio. To integrate the volumetric ratio between fluid and solid for velocity calculation it is assumed that the actual viscosity is between the viscosity of water and the “viscosity” of unconsolidated clastic material (interpreted to behave like a highly viscous liquid). A further assumption is that the change of viscosity is linearly proportional to changes of the solid/water volume ratio:

$$r_{sol/water} = V_{sol} / (V_{sol} + V_{water}) \tag{8}$$

V_{water} volume of water [m³]
 V_{sol} volume of solids (particles) [m³]

Several authors like Krieger and Dougherty (1959), Chen (1986), Amy et al. (2005) have shown that viscosity of fluid–particle mixtures

depends to a great extent on the ratio between the volume of the particles and the volume of the fluid. If the particle volume is less than 50%, the viscosity changes due to particle volume can be roughly approximated with the linear equation shown, or even better with power laws (Chen, 1986; Fig. 2).

3.5.2.5. Integration of slope and friction. The velocity of a viscose liquid running down an inclined plate as dependent on time can be written as:

$$v = v_0 + \Delta t g \sin \alpha + \Delta t F_R / m + f_{sc} \Delta t F_I / m \tag{9}$$

F_R $gm\mu\cos\alpha$ (surface friction)
 F_I $6\pi\eta v_0$ (internal friction)
 v_0 initial velocity [m/s]
 g acceleration (due to gravity) [m/s²]
 α slope [°]
 μ friction factor [–]
 m mass [kg]
 η dynamic viscosity [Pa s]
 f_{sc} scaling factor [–]

To describe internal friction Stokes law is applied (slow movement of particles in a viscose medium (for higher velocities internal friction is proportional to the square of velocity).

To simplify the handling during simulation Eq. (9) was changed to:

$$v = v_0 + \Delta t g \sin \alpha (1 - \mu) + f_{sc} \Delta t F_I / m \tag{10}$$

As a consequence the mass flow will act similarly to a Newtonian liquid. As the value of the term $\Delta t 6\pi\eta v_0 / m$ of Eq. (9) increases with speed, the mass flow will reach a maximum velocity which is used as the characteristic velocity for the specific situation (local slope, fluid/solid ratio). We calibrated the formula with using real world measurements conducted by various authors (Table 1).

Using the measured values a slope-dependent correction for the friction factor (μ) was introduced (results greater 1 are replaced with 1), assuming that channels in mountainous areas are characterized by higher surface friction:

$$\mu = 1.21 * \ln(\alpha) + 0.5239 [---] \tag{11}$$

We used the dynamic viscosity of water, 0.001002 (20 °C, 1 bar). The amount of transported sediment is adjusted automatically depending on the transport velocity.

3.6. Time dependent environmental parameters

Several environmental parameters were altered in dependency of time during the process of simulation.

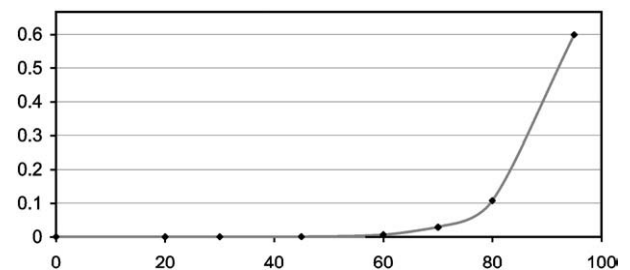


Fig. 2. Viscosity of mixture fluid and cohesionless particles (Krieger and Dougherty, 1959), fluid viscosity is set to 0.001, “viscosity” of particles is set to 1. x-axis: particle concentration, % of volume. y-axis: viscosity, kg m^{–1} s^{–1}.

3.6.1. Precipitation factor

The amount of available water influences the simulation in different ways:

- Increasing stream power.
- Ratio between transported sediment and water may change which will influence transport speed and deposition.

3.6.2. Sediment supply factor

The sediment supply factor is an additional time dependent factor, which allows adding a time dependent behaviour (by multiplication with the transport coefficient). This factor is not connected to a certain chemical, biological or physical process. In the work presented here this factor was used to model climatic changes and related processes such as change in vegetation coverage and impact of weathering.

3.6.3. Tectonics

In WinGeol/SedTec tectonics is treated as a passive process. Rates of subsidence or uplift are user input-derived and are not influenced by the simulation results.

Rates are read from a separate (time) table, which is linked with a polygon element. Each element may have different rates and be activated as often as needed.

4. Reference model, modelling approach

We calibrated a reference model (1a, 2a, 3a; [Table 2](#)) to the natural system which fits best to the present Mitterndorf Basin fan geometries and produces comparable fan thicknesses at the end of the modelled time span of 25 ka. Calibration data were mainly gained from outcrops, drill logs and geophysical data such as geoelectric, seismic and Bouguer gravity surveys ([Küpper, 1950](#); [Havinga, 1972](#); [Salcher, 2008](#); [Salcher and Wagreich, in press](#)). The reference model was used to better interpret results from the numerical experiments in terms of deviations from the reference models.

In the natural system the last aggradation event on both fans can be constrained to the Last Glacial Maximum around 20 ka B.P. This period was modelled via high sediment supply and reduced discharge values ([Fig. 3](#), exp. 1). Incisions of the Mitterndorf Basin interfan channels took place around 12 ka ([Salcher and Wagreich, in press](#)). The climatic recovery since ca. 11.5 ka (End of the Younger Dryas; [Oldfield, 2005](#)) was modelled via a continuous, linear decline in sediment supply and a coeval increase in precipitation values ([Table 2](#)).

Subsidence rates of the reference model are set to values known from precise levelling measurements ([Höggerl, 1980](#)) by default.

In exp. 1, the sediment supply values were altered to higher and lower values compared to the reference model. In exp. 2, subsidence values were set to zero, to low and to extreme values (4 times the reference model value) compared to the reference model. Effects of base-level fall (incision) were modelled in experiment 3. Our models cover a period of 25 ka with 8 time steps. Hence, each time step records 3125 years ([Fig. 3](#)).

Our models do not incorporate different rock types as changes in bedrock are very low over all the study area and consist almost entirely of Triassic carbonates (Northern Calcareous Alps).

Table 1
Comparison of measured and calculated flow velocities.

Vol.% sed	Slope (degree)	μ friction factor	Mean velocity (m/s)	Reference velocity (m/s)	Source of measured data
0.015	0.1	0.25	1.08	1	Schulze et al., 2005
0.15	–	0.9	5	~4–5.4 (max. v)	Hodel and Lehmann, 2000
~0.02	0.22	0.34	1.75	~1.0–2.0	H. Habersack, 2005

4.1. Preparation of the initial model

Landscape evolution models which simulate changes over a geologic time scale and large areas have to be simplified due to limited computation power. Therefore, the initial models have to be optimized and simplified (e.g. [Allen and Densmore, 2000](#); [Clevis et al., 2003](#); [Cowie et al., 2006](#)). The spatial resolution of the original DEM grid cells (10×10 m) were reduced to 150×150 m or 200×200 m respectively. The model combines the natural elevation data of mountain catchments with a virtual basin surface grid. The virtual surface represents a tilted plane simulating the mean slope (~0.1°) of the recent southern Vienna Basin (which includes the Mitterndorf Basin) to NE. It offers the opportunity to evaluate fan and basin development without morphological structures like incised streams, gullies, depressions caused mainly by anthropogenic features like artificial river channels, dams, railroad tracks, highways and gravel pits. Furthermore, a present day basin surface grid is not supposed to be appropriate as aggradation cycles are taking place after a long time of fan abandonment and degradation. The simulated fan growth is therefore not affected by the present day topography but by a flat tilted surface which better allows the fans to evolve and to be interpreted within the set frame-work conditions.

4.2. Local depression handling

We used a cycle prior the simulations to fill up artificial local depressions of the natural (mountain catchments) DEM. Results of this cycle were analyzed to be sure that geometrical alterations stay minor. However, in proximal fan areas, sequence aggradation on fan surfaces was shown to be immoderately large at the end of time step 1. This is a filling effect of the first calculation cycles of time step 1 caused by the transition gap from the natural DEM (Alpine Hinterland) to the artificial flat plan of the basin. This gap could not be removed by the cycle prior to the simulations.

5. Results

In this study we generated 12 models to investigate the effects of different combinations of input variables ([Table 2](#)).

5.1. Experiment 1 – variations in sediment supply

In order to evaluate the influence of variations in sediment supply and precipitation rates on fan evolution, we created models that simulated the consequences of strong climate change during 25 ka by tuning discharge/sediment ratios ([Fig. 3](#)).

The models of experiment one are simulated via changing sediment supply affected by colder (more sediment input, model 1c and 1d) and warmer climate (less sediment input, model 1b) than the reference model. Discharge values simulating cold (less precipitation and discharge values) and warm periods (higher precipitation and discharge values) stay constant in all models. Values are allowed to develop with sediment supply rates transporting –50% (1b), +100% (1c) and +400% (1d) of the reference model (1a). Tectonic slip rates were held constant and the influence of neighbouring axial river (Danube) on base level were censored.

In model 1b, our results indicate that the decreased availability of sediment leads to increased stream power per unit bed width (higher discharge/sediment supply ratios), causing both high sediment conveyance capacity and high rates of bed rock erosion ([Fig. 4](#)). In proximal fan areas, model 1b was not even accumulating to end of the simulated full glacial up to time step 5.

Lower availability of sediment was found to be associated with lower sequence thickness, lower channel activity on the fan surface and a higher sensitivity to subsidence. Models with low sediment availability are not effectively able to balance progressive formation of

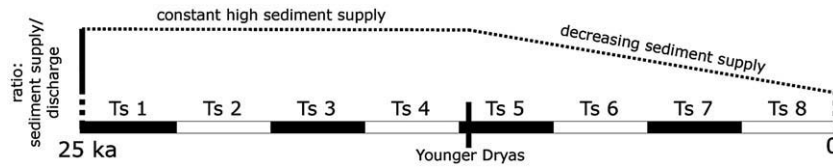


Fig. 3. Simulated time span of 25 ka divided into 8 time steps. Applied curve of sediment supply as a ratio of sediment supply divided by discharge.

accumulation space through subsidence. Main channels are deflected towards highest subsidence areas in the centre of the basin. Low sediment supply in model 1b allows only very minor deposition on the upper fan. Little sediment is preferentially stored in the distal fan areas (Fig. 6a). The decreased sediment supply rates are associated with high rates of stream incision, which is even more increased towards the end of the model runs, where sediment/discharge relations are lowered (Figs. 3, 6, 7). The deeper incised river networks show a higher stability during the later simulation steps – incision is maximized within a rather small number of channels.

In the models 1c and 1d, higher availability of sediment was found to cause higher sequence thicknesses, some longer fan progradation distances, an increasing number of channels on the fan surface, different runoff patterns and generally less influence of subsidence. The overall reduction of sediment aggradation on the fan surface, which is observable in all models even before time step 5 (Fig. 6a, up to time step 5 constant values of sediment are delivered to the fans) is a function of critical slope. If critical slope is reached sediment is delivered to more distal positions, i.e. fans prograde. Because of the higher sediment supply, incision is rather small (the transport medium is not able to take up more material) and therefore the channel network shows a greater variability in time and space.

In models with abundant sediment supply, subsidence is balanced more effectively, resulting in a different flow pattern which is not effectively influenced by the subsiding areas. Aggradation behaviour on the fan surfaces during the simulation is similar in models 1c and 1d. Up to time step 4, aggradation occurs in the upper fan regions. With time step 5 (lowering of sediment supply) aggradation preferentially occurs in outer fan positions. The decreasing amount of sediment is forced to fill high subsidence areas in distal positions preferentially. Generally, the abundant sediment supply led to multiple channel development where channel incision is very restrained during all time steps. With time step 8, minor incision causes some small areas in upper fan positions to be abandoned and are not affected by deposition (Fig. 4). Abandoned areas are generally larger on the Piesting fan, because streams tend to level out in a NE direction, not eroding the fan surface.

In all models the southern Schwarza fan is affected by a larger number of channels which is especially obvious in model 1b (low sediment). In summary, climate-induced variations of sediment supply have a strong impact on fan aggradation and morphology. Abundant sediment supply allows thicker sequences to develop, resulting in larger fans and valley backfilling which corresponds to a fan apex at a higher elevation. Models with high sediment supply show lower bedrock incision, numerous but shallow channels and low sensitivity to subsidence. Low sediment supply produces smaller fans, allows higher bedrock incision, resulting in fewer but deeper channel

systems and results in a higher sensitivity to tectonic subsidence. In our models a higher channel density reflects an active fan surface or active depositional lobes showing reduced incision and a higher avulsion tendency (Figs. 4, 5). High channel density on the lower parts of the fans can be equated with intersection point shifting distally and the loss of accumulation space relating to low sediment supply rates. High channel density on extensive areas of the fan can be equated with a intersection point closer to the apex and high accumulation space (open fan deposition) relating to abundant sediment supply rates. Active depositional lobes are represented by high-slope areas, because numerous flow (transport) events produce numerous channels with relative steep banks. These channel banks show a high colour contrast, which is visible in a slope distribution map (Fig. 5). High-slope areas on fan surfaces also develop in our models, e.g. through distally eroding or confining processes (erosive scarps). Low slope areas on the fan surfaces show sediment congestion (laterally fan confinement, e.g. at the Alpine front) or an abandoned fan surface (no channel development). The tendency for interfan channels on the Piesting fan to deflect towards the NE is an effect of the overall basin slope.

5.2. Experiment 2 – responses to changes subsidence rates

In order to better understand the consequences of faulting and developing accumulation space on alluvial fans in the Mitterndorf Basin, we created models with different subsidence rates. The elongated basin is about ~270 km² and trends SW–NE. The natural basin is highly active (Decker et al., 2005), known to have subsided since the Middle Pleistocene at around ~250 ka B.P. (Salcher, 2008). The northern part of the basin is narrow (<2 km) filled up with up to 170 m thick alluvial gravels. An average slip rate of 0.7 mm/a can be assumed for the deepest basin parts (170 m) over 250 ka. Alluvial fans fill the up to 10 km wide southern part with more than 100 m of massive gravels and thin palaeosol sequences (Salcher and Wagreich, in press). Basin filling declines from North to South, and from the mountain front in the West to the East showing some asymmetry in basin form. Maximum slip rates can be assumed in the East and North of the basin (Hinsch et al., 2005; Salcher, 2008). Precise levelling data indicate subsidence rates of approx. 1 mm/a (Höggerl, 1980). The difference in subsidence is simulated by a defined fault map (via a set of polygons) with lowest slip rates in the West close to the mountain front and maximum rates in the East of the Basin (Fig. 1). Slip rates were held constant for each subsiding polygon during a simulation run.

In experiment 2, the ratios of precipitation and sediment supply are held constant, whereas fault slip rates vary: model 2a serves as reference model (slip rates reflect precise levelling results with a maximum of 1.2 mm/a; Höggerl, 1980; Table 2). Model 2b is characterized by tectonic quiescence (0 mm/a), model 2c develops with low subsidence (max. rates are 0.3 mm/a), model 2d with medium subsidence (max. rates are 0.6 mm/a) and model 2e with fast subsidence (max. rates are 2.4 mm/a; cf. Decker et al., 2005). For further simplification, we did not take strike-slip movement into account, which is in the range of few mm/a (Decker et al., 2005).

In model 2b, the Piesting fan builds a radial form extending to the NE, only confined in the southeast by the prograding Schwarza river fan (Fig. 7). At proximal positions aggradation is higher than on

Table 2
Parameters used in the reference model.

Reference model	Time (ka)	Sediment supply	Precipit.	Subsid., area V, distal: (m/ka)	Subsid., area I, proximal: (m/ka)	Time step
1 a, 2 a, 3 a	25–11.5	0.3	0.15	0.075	1.2	1–4
	11.5–0	0.1	0.5	0.075	1.2	5–8

Changes in sediment supply and precipitation are not abrupt but increase linearly. For location of subsidence areas see Fig. 1.

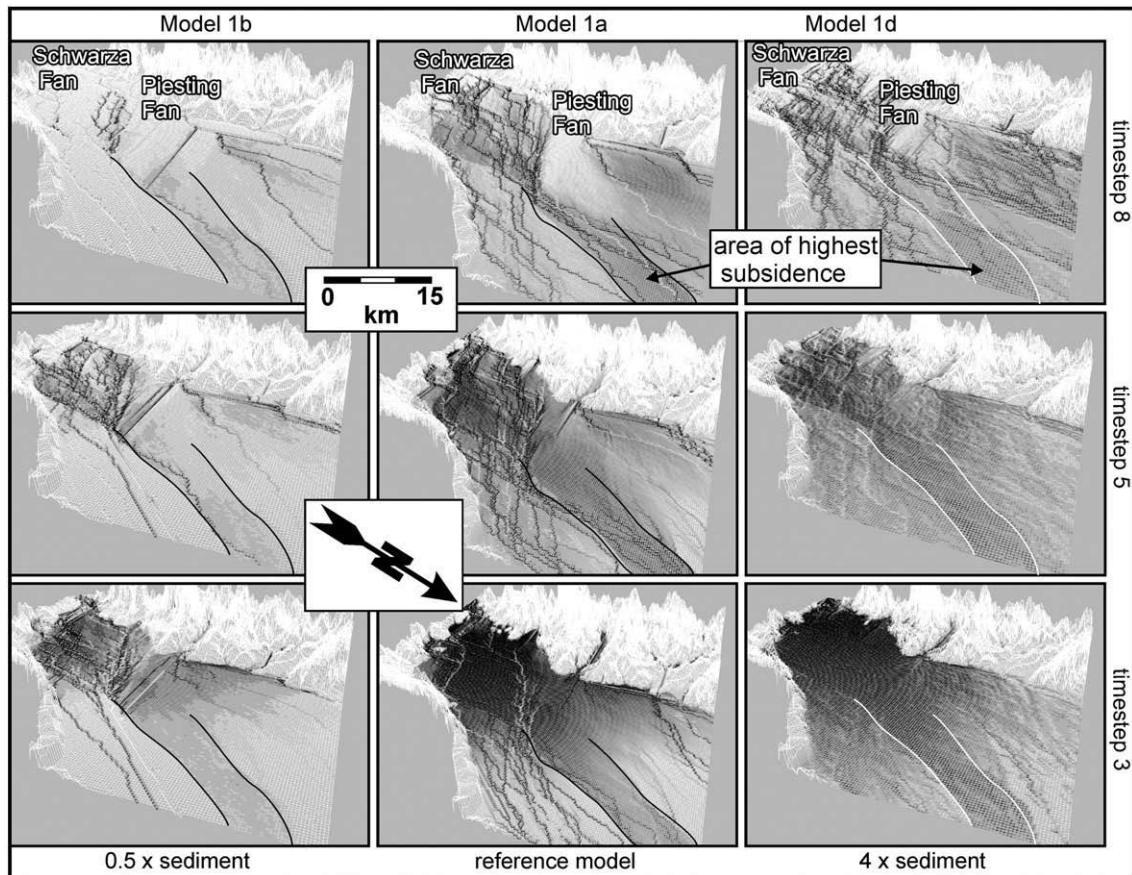


Fig. 4. Influence of sediment supply variability within the study area. Low supply models (1b) are strongly influenced by the basin's high subsidence areas in the central parts. Channels are able to incise deeply, especially during simulated warm periods, leaving large abandoned fan surfaces at the end of model runs (time step 8). High sediment supply (1d) causes large aggradation on fan surfaces during the first time steps, weak tectonic influence and a multiple network with shallow channel. All models show the difference in aggradation, Schwarza to Piesting Fan. The southern Schwarza Fan is affected by higher aggradation but also by stronger degradation. Reference model (1a) shows a, compared to the nature, realistic drainage network evolving and realistic fan area sizes during the end of model run. Black colour represents thicknesses of more than 10 m; white colour represents no accumulation on cell. Black and white lines frame areas of highest subsidence. Grid space is 200 m, vertical exaggeration is 20 times.

models with high subsidence (Fig. 7). The absence of subsidence does not force channels to incise and aggradation is not drawn to these areas. Progradation is then just an effect of critical slope. Aggradation increases more or less linearly with distance from proximal to distal fan locations.

Effects of sediment reduction with time step 5 lead to interfan channel incision and to the abandonment of the fan surface in all models. Interfan main channels of low (2c) or no tectonic model (2b) series level out in a N–S direction (along or near the Alpine front) with increasing time and decreasing sediment supply. The direction of aggradation of these models is mainly influenced by the overall basin slope which is to NE. Due to the conical form of the fan, the interfan channels shift from higher points to a lower position which is the case for the non-normal tectonic models always near the Alpine mountain front. The resulting abandoned fan surface during warm periods for the Piesting fan appears very large and is not at all comparable to today's geometry. Fans affected by low or no tectonic activity create less accumulation space than fans affected by high subsidence rates. Fans develop smaller thicknesses. Models with lower subsidence rates show a longer fan activity in their proximal areas (time step 6 and 7) because incision is not (or only minor in case of model 2c) affected by additional subsidence (which becomes relatively more important during simulated warm periods with time step 5). In contrast, increasing subsidence rates in distal areas (2d, 2e) prolongate the fan activity in response to the developing accommodation space.

In model 2d and 2e, the response of the catchment fan system to the increase in fault activity is reflected by the evolving fan geometry and channel evolution on the fan surface (Fig. 7). Models with high

subsidence rates fill subsidence areas, cause main channels to level out towards maximum slip rates earlier (Fig. 7). This effect is amplified as sediment supply decreases and accumulation is deflected to the depocenter of the basin. During periods of fan build-up extreme subsidence rates in 2e produce conspicuous fan forms, which are elongated towards the maximum subsidence area. Progradation distance and geometry is shown to be directly in dependent on tectonically created accommodation space. Already with time step 4, most sediment is accumulating in high subsidence areas in distal fan locations. With the beginning of low sediment supply (time step 5) the effect of constantly high vertical slip rates amplifies channel incision and channel confinement (Figs. 6, 7).

As in the experiment 1, the channel number is clearly higher on the southern Schwarza fan preventing an abandoned fan surface from developing.

In all tectonic models (2a, c, d and e) in which the fans are affected by lowering through subsidence, progressive creation of accumulation space causes burial of old fan sequences rather than erosion (2c and 2e). Lowering of fan areas due to subsidence, enables (axial) streams to reoccupy these areas and force streams to fill the space. The higher the vertical slip rates (2c to 2e) the more sediment is delivered to the maximum subsidence area, and the higher is the tendency for streams to aggrade. The large amount of accumulated sediment in these high subsidence areas is reflecting very minor erosion which can be associated with high sequence preservation potential.

In the study area this subsidence effect is characterized by the occurrence of paleosols, which are thicker and more frequent in the basin centre (Küpper, 1950; Salcher and Wagreich, in press).

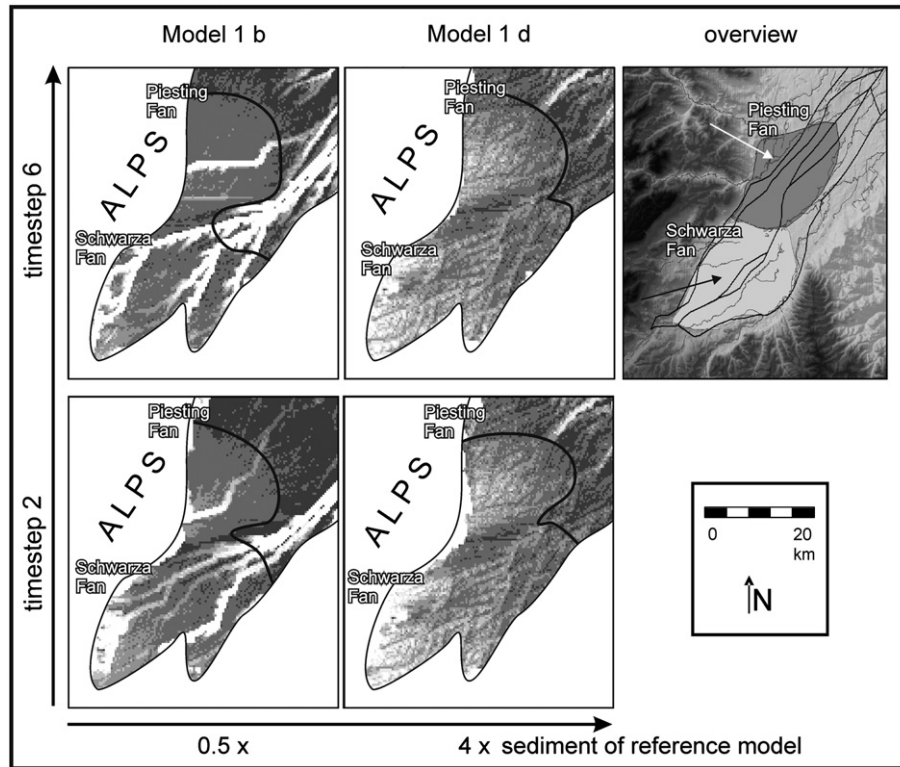


Fig. 5. Slope map of model 1b and model 1d, showing the impact of low and high sediment supply on models. White colour indicates high slope ($>1^\circ$, deep incised channels), black indicates low slope (0°). Low sediment transport to the basin (1b) cause strong incision into fan surface producing steep channel banks. Models with high sediment supply have to disperse their sediment on the surface creating abundant but less deep channels.

5.3. Experiment 3 – river level fluctuations of the main axial river (Danube)

The investigated fans toe out onto the subsiding Mitterndorf Basin. Streams of the basin are also influenced by the level of the axial Danube River to which all streams are tributary. The level of the Danube River may alter due to fluvial incision or accumulation. The Danube River acts like a conveyor belt which gathers all sediments from Vienna Basin tributaries. Therefore, the water level is climatically influenced.

In experiment 3, the impact of a main river onto local base level and thus fan development during the sequence of 25 ka is observed. Streams are allowed to drain to different elevation levels at the model's edge, simulating the effect of incision of the Danube River. Within this experiment sediment supply and subsidence rates are held constant (values correspond to the reference model). The reference model is 3a. Average distance to base level is changed to -15 m in model 3 b. For simplification base-level variations within model runs held constant.

In model 3b the water level of the main river is set to lower positions (some 15 m below the present Danube level) resulting in strong incision (Fig. 8) and suppression of fan development. In proximal fan areas, aggradation occurs up to time step 2 on the Piesting fan, but almost completely ends at time step 3 (Fig. 6c). A wave of dissection which propagates upstream reaches the fans and lead to total fanhead trenching preventing accumulation on the upper fan surfaces, which are then completely abandoned. However, if accommodation to that base level is finished, models allow a constant aggradation on the distal fan parts even when sediment supply decreases with time step 5.

6. Discussion

In a steady-state landscape the fan area-catchment relationship is in theory almost entirely determined by the tectonic setting, if no significant alteration in climate or source lithology occurs (Whipple

and Traylor, 1996). The total amount of time required to re-establish a steady state after perturbation depends on the strength of the climatic impact: if much sediment is provided to the fans, landscape re-establishment may take a longer time, if less sediment is supplied re-establishment time is shorter.

The study area fans respond to short climatic events in the range of only some 10^3 with strong, transient pulses of sediment depicting the primary control on fan evolution (c.f. Nemeč and Postma, 1993;). After that massive impact, alluvial fans become inactive and subsidence is the main controlling factor on where sediment is distributed (Ritter et al., 1995).

6.1. Sediment supply

In exp. 1 variations in sediment supply were carried to study fan activity time, evolution of fan form, fan surface preservation and behaviour of interfan channels.

A decrease of sediment supply to a half of reference models shows that fans which are starving of sediment have a higher sensitivity to subsidence. The sediment pulse which provides only low sediment from the catchment to the basin overwhelms the tectonic impact only during a short time span (up to time step 3, Model 1b). In areas of high subsidence, once channels have become entrenched they are not able to leave these areas. The number of channels is generally reduced and bed incision values are higher (Figs. 3, 4).

Models with high sediment supply evolve a "braided" pattern to distribute abundant sediment on the fan surface. Channels are numerous and channel incision is clearly restrained which leads to a higher lateral erosion potential (cf. Vandenberghe, 2008). Especially towards the end of simulation (time steps 6–8), fan geometries are importantly influenced by lateral erosion processes. Models with high sediment supply stay decoupled longer from the axial trunk stream (model's edge) and take longer to approach to a steady state.

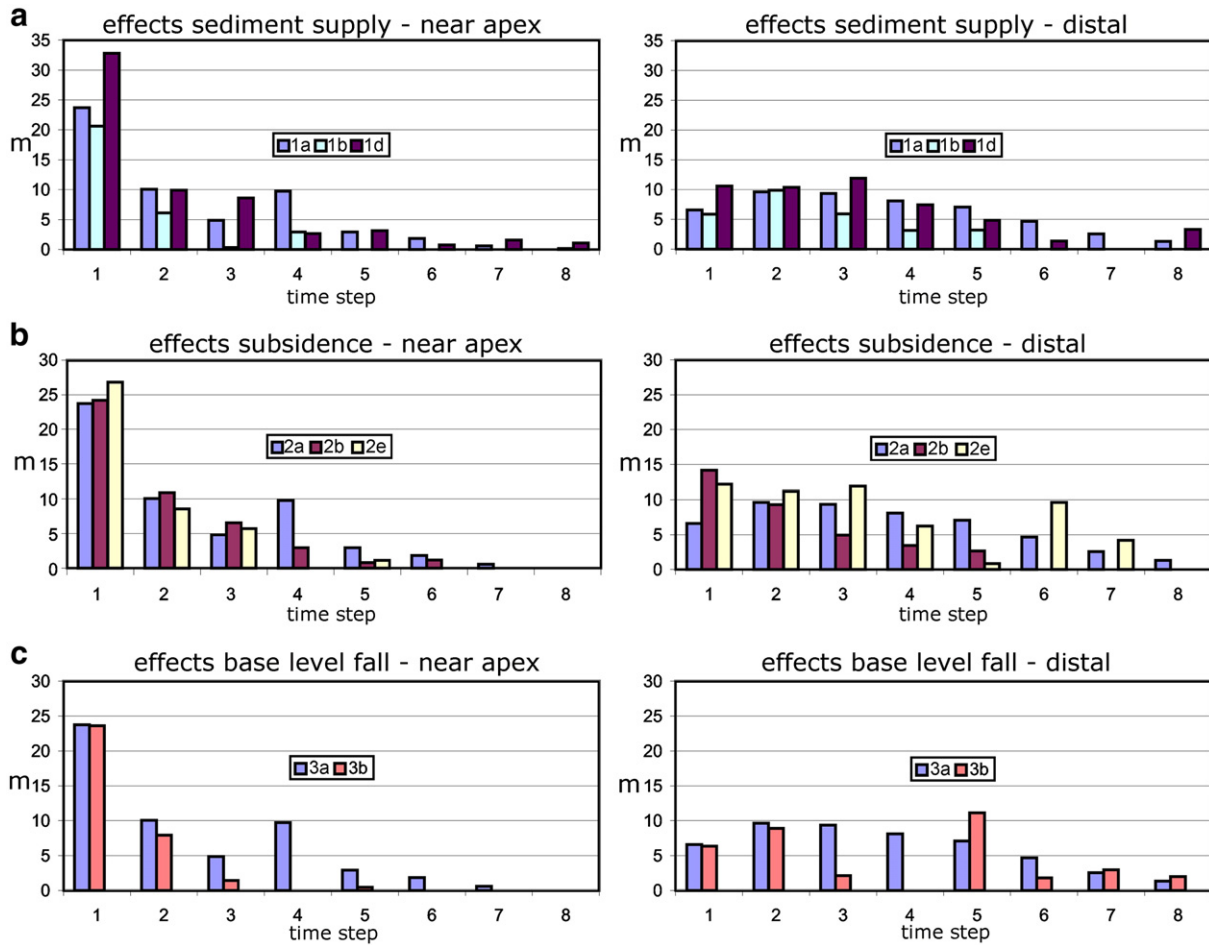


Fig. 6. Virtual wells show the amount of aggradation (in m) on Piesting fan near the apex and on a distal position at the end of a simulation (showing the remained sediment after each time step). At proximal positions, strong aggradation during time step is a filling effect at the transition of the natural DEM Alps to virtual Vienna basin DEM (see 4.2). Experiment 1 model series show the effects of sediment availability. (a) Experiment 2 model series show the preservation potential between no, normal and high subsidence rates. (b) Experiment 3 model series show the effects of a lowered base level. (c) All models show the clear decline at time step 5 at simulated warm periods (increasing discharge/sediment supply values). For location of virtual wells see Fig. 1. See text for further details.

Generally, variations in sediment discharge does not only control fan volumes or sizes but also largely influence the evolution of a drainage network after simulated climatic disorientation. It determines the erosion potential of both fans and therefore the sequence development.

6.2. Subsidence

As typical for pull apart basins (e.g. Wu et al., 2009) the highest subsidence rates are not close to a main thrust fault as in e.g. half graben settings or in a foreland basin). The highest subsidence rates of our models are in the north and east of the basin mimicking the actual basin kinematics. Evolution of highest accommodation space is therefore not at the mountain front but rather in the distal areas. The more or less constant basin subsidence since c. 2.5×10^5 years has an effect on the creation of accommodation in a long term sense.

Gordon and Heller (1993) suggest that differences in subsidence may explain much of the variability recorded in modern fans. The importance of the spatial distribution of basin subsidence areas and fan volume and size has been pointed out by Whipple and Trayler (1996).

Our models show fan accommodation to subsidence areas during a relative short time span (c. 10 ka). Subsidence becomes more effective at the end of model runs where simulated warm periods provide a generally lower sediment input. Fan progradation distance increases with time if subsidence rates return to higher values. This may wonder

as lower subsidence results are generally associated with larger fans and higher subsidence with smaller fans (e.g. Viseras et al., 2003). The reason here might be that high subsidence areas primarily affect distal fan parts and are not located in proximal positions like at a typical mountain-front fan setting. Evolving accommodation space force sediment streams to aggrade preferentially in these locations. Fan channels are affected by the location of the highest subsidence areas. The higher the subsidence rates of the basin, the higher is the ability of channels to incise into the fans and the lower is the ability of channels to incise into the floodplain (in the north of the basin). A clear analogy in the natural study area is the tectonic sag pond, with highest subsidence rates in the northern basin (Decker et al., 2005): numerous flooding events are evident in the historical and stratigraphical record (Salcher and Wagreich, in press) – terraces are generally missing.

As subsidence becomes relatively more important during its way to a steady-state landscape (cf. Adams, 1980; Molnar and England, 1990) the evolving drainage system towards the end of simulations differs clearly depending whether the basin is not, is little or highly affected by subsidence. In our models this results in a totally different pattern of incipient location of channel incision, and thus, fan erosion.

In case of the Schwarza fan, tectonic quiescence forces streams to follow the preferentially overall basin slope to the NE. The Piesting fan develops an ideal radial fan form during the absence of subsidence. Its steepest slope develops more or less normal to the fan axis close to the mountain front, forcing channels to shift towards this direction. After they have left the alluvial fan area, they follow the overall basin

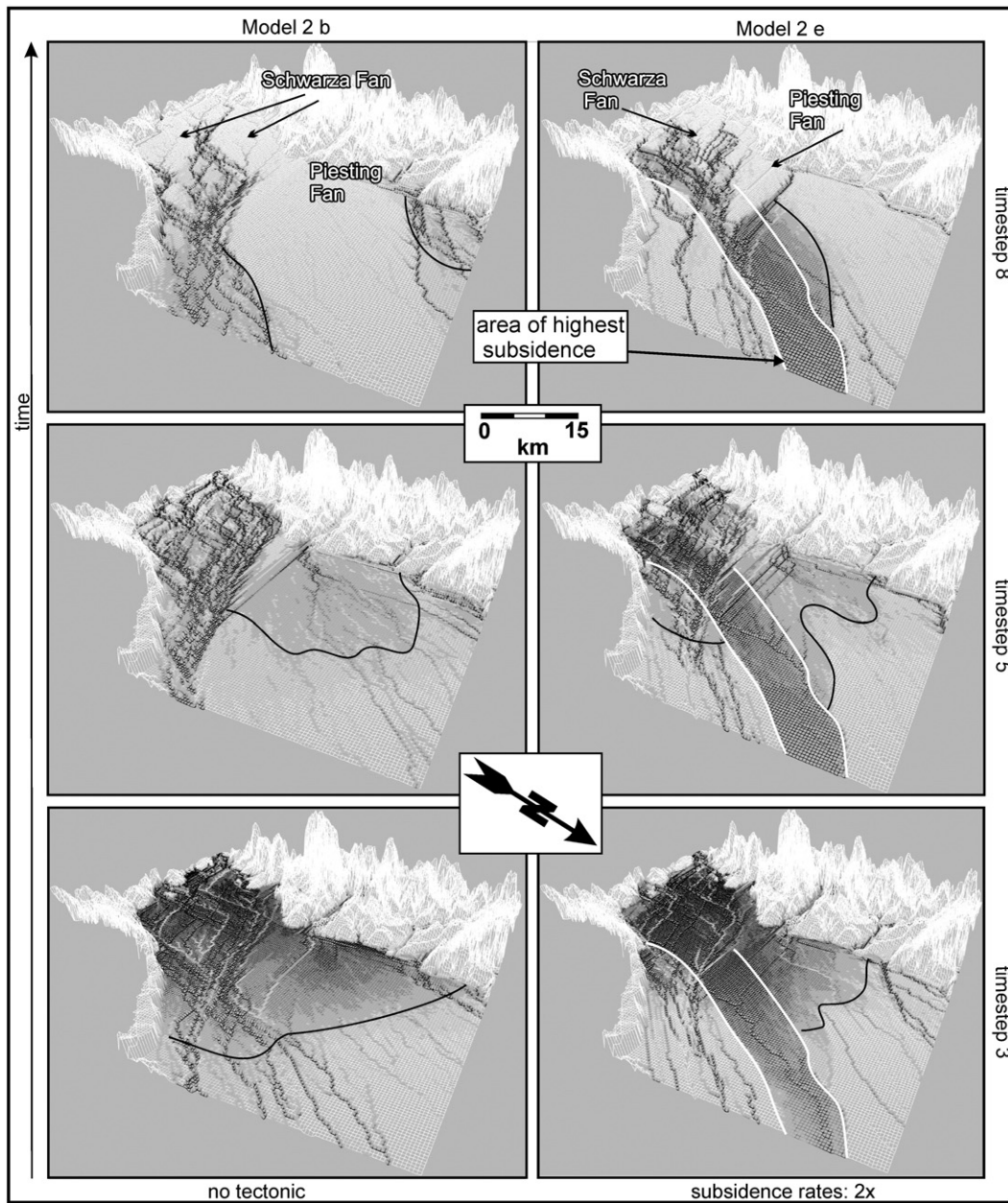


Fig. 7. Influence of basin subsidence (model 2e) and tectonic quiescence (model 2b) on fan evolution, showing the development of the stream pattern. Black colour represents thicknesses of more than 10 m; white colour represents no accumulation on cell. Channels appear often dark, showing a high amount of sediment passing individual cells per time step (high sediment flux). Note the progressive filling of high subsidence areas. Grid space is 200 m, vertical exaggeration is 20 times.

towards the NE. The preserved fan surface is very large and not comparable to today's geometry. In contrast, if subsidence is turned to extreme values (2d, 2e) the Piesting fan is eroded by interfan channels of both fans which got diverted into the areas of highest subsidence. The resulting fan surface is very small. In-between, the reference model 2a serves a realistic form, very much comparable with today's fan geometry where fan abandonment through incision and levelling out of the natural Piesting River to a NE direction can be constrained to c. 10 ka B.P. (Salcher and Wagreich, in press).

Our models show that both variation in sediment supply and subsidence rates may have large impacts on stream evolution and therefore exert an important influence on the preservation of sequences.

If the landscape is re-establishing after climatic disorientation, subsidence becomes the primary variable in our fan environment again. In accordance with the model of Ritter et al. (1995) for

mountain-front fan evolution in SW Montana, we suggest that ongoing subsidence does progressively produce a suitable environment for alluvial fans to accommodate in the next phase of high sediment discharge and fan formation.

Focusing on the differences between the two fans, models of exp. 1 and exp. 2 show clear differences in channel activity: the Schwarza fan is affected by a much higher number of channels than the Piesting fan – throughout all the simulation runs. Its catchment provides more sediment supply to the fans. Through its lateral alpine confinement and some lower subsidence rates, sediment reworking processes are higher. Hence, the fan is much later or even never completely abandoned. The erosion potential of the Schwarza fan can be stated to be much higher.

The comparison with the natural fans shows in fact that fans have a different preservation potential: soils which evolve during times of fan

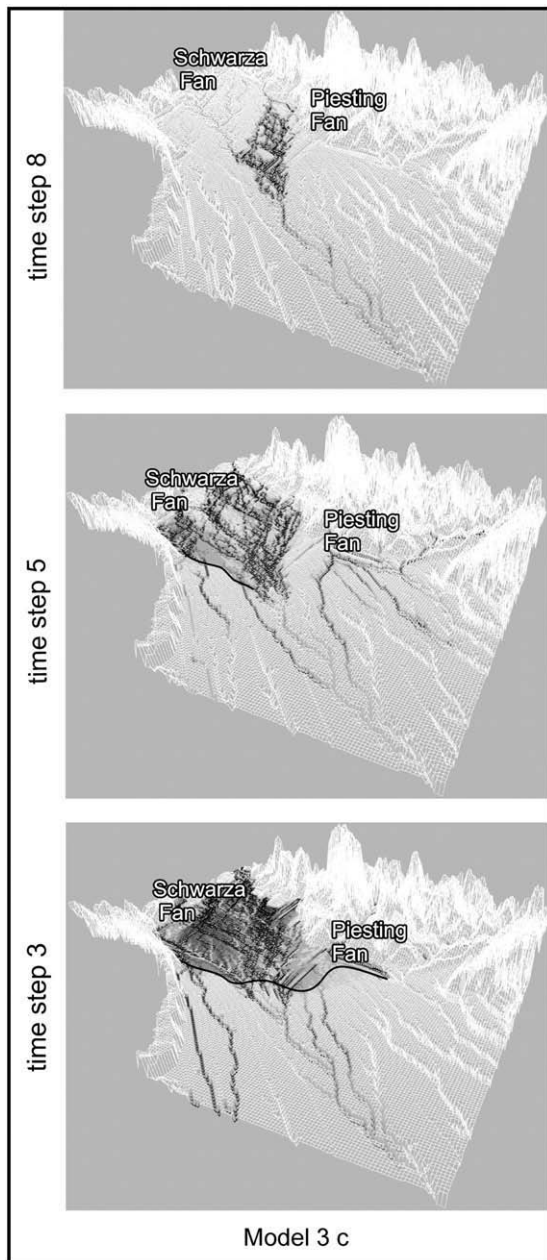


Fig. 8. Extreme lowering of base level in model 3c shows the strong incision of Danube River tributaries into bedrock and the suppression of fan progradation. Black colour represents thicknesses of more than 10 m; white colour represents no accumulation on cell. Grid space is 200 m, vertical exaggeration is 20 times.

inactivity on fan surfaces are often eroded and less common in the Schwarza fan sequence than in the Piesting sequence.

The incision of this channel (Piesting River) into a NE direction following the overall basin slope correspond very much with nature. Almost all models show the same trend except models which have extreme subsidence rates (2d and 2e) where interfan channels do not leave the highest subsidence areas at the end of simulation runs.

6.3. Base level

The influence on base level by a neighbouring axial main river is computed in experiment 3. Lowering of the axial main river causes incision and upstream dissection through tributaries in our models. Responses to a base-level fall are fast, causing a wave of dissection

which propagates from the main river to the upper basin parts. Fan development is suppressed but depends on the amount of main river incision (lowering) and on sediment supply. Similar to experiment 2 abundant sediment supply suppresses trenching tendencies, while decreasing sediment supply values towards the end of the simulation result in formation of deep fan trenches. Nevertheless, in the natural situation, strong base-level alterations of the kind simulated in our model are unlikely, as within this specific time frame water level can be assumed to have been relatively stable. Fluctuations in elevations of the Danube River are very minor (Fink, 1955). The elevation of terraces of the late Middle Pleistocene (MIS 6, Riss age, some 130 ka) above the contemporary floodplain of the Danube does not exceed c. 15 m, demonstrating generally very low incision. Therefore, experiment 3 is of rather hypothetical interest and results can only be applied with caution.

6.4. Strength and limitations of simulated landscape models

The program code used was sensitive enough to explain the geomorphic evolution of our study area. We were able to generate realistic fan geometries, drainages and could detect the most probable factors controlling Mitterndorf alluvial fan and sequence evolution. Landscape evolution models which simulate changes at a geologic time scale and over large areas have to be simplified due to limited computation power and limited information on relevant processes of the investigated area (e.g. Clevis et al., 2003; Cowie et al., 2006). We did not include very short (e.g. Younger Dryas) climatic oscillations which might have led to a further pulse of sediment supply. Environmental parameters such as weathering and grain size reduction were excluded.

7. Conclusion and outlook

Our numerical models simulate fan build-up and degradation as dependent on dependence of subsidence and base-level fall during a simulated glacial/interglacial cycle (25 ka–0). A reference model was calibrated to the real world and used to define significant alterations to the reference real world scenario. Models show that the alluvial fan development is primarily affected by distinct sediment supply pulses during phases of short climatic perturbations. During that time the tectonic signal is overwhelmed, but becomes the determining factor again when models approach a long term steady state.

The variations in sediment supply (Exp. 1.) show that the evolution and determination of the drainage network during simulated warm periods is significantly influenced by whether supply rates are high or low. Similarly, variations in vertical slip rates of faults (Exp. 2) do affect the long term evolution of the drainage system. Both factors significantly control the sequence preservation potential of fans and therefore the long term sequence evolution. Basin slope is another prominent factor influencing drainage evolution especially if vertical slip rates are low. The lowering of the axial main river elevation has a strong and fast impact on all tributaries of the drainage basin. Sedimentation on the fan is suppressed. Fan confinement and catchment also play important roles on fan evolution and the erosional potential of fan deposits. The confined Schwarza fan is affected by stronger aggradation but also by stronger degradation processes in contrast to the Piesting fan.

Thus, our models help to better understand fan development and controlling factors, i.e. the control and evolution of the drainage system, sequence development and preservation potential of fan deposits. Essentially, our models act as landscape evolution models (e.g. Allen, 2008).

The software might also be used to simulate sediment fluxes over a much shorter time span helping to better understand and predict catastrophic events on fan surfaces. Consequently, our models may allow a primary evaluation of the risk of flooding events in the area.

The Schwarza fan does generally show a high channel avulsion tendency – especially when sediment flux is set to high values: the sediment routing system tends to be instable and may cause some higher catastrophic flood potential than the abandoned Piesting fan. Drainage on the Piesting fan is influenced by the overall basin slope to the NE. In fact, crevasse splays and overbanks fines along the natural Piesting River indicate recurrent flooding events there. Similarly, drill logs and historical records show increased flooding potential along the highest subsidence areas in the north of the basin.

Acknowledgments

This project was funded by the Austrian Science Foundation (FWF Project AP18203). We thank Belinda Plattner for help with the manuscript write-up. We further acknowledge Stuart J. Jones and anonymous reviewers for their very helpful and critical comments on the manuscript.

References

- Adams, J., 1980. Contemporary uplift and erosion of the Southern Alps, New Zealand. *Bulletin of the Geological Society of America* 91, 1–114.
- Allen, P.A., 2008. From landscapes into geological history. *Nature* 451, 274–276.
- Allen, P.A., Densmore, A.L., 2000. Sediment flux from an uplifting fault block. *Basin Research* 12, 367–380.
- Allen, P.A., Allen, J.R., 2005. *Basin Analysis*. Blackwell, Oxford.
- Amy, L.A., Peakall, J., Talling, P.J., 2005. Density and viscosity stratified gravity currents: insights from laboratory experiments and implications for submarine flow deposits. *Sedimentary Geology* 179, 5–29.
- Andrews, D.J., Bucknam, R.C., 1987. Fitting degradation of shoreline scarps by a nonlinear diffusion model. *Journal of Geophysical Research* 92, 12,857–12,867.
- Anderson, R.S., Humphrey, N.F., 1990. Interaction of weathering and transport processes in the evolution of arid landscapes. In: Cross, T.A. (Ed.), *Quantitative Dynamic Stratigraphy*. InPrentice-Hall, Englewood Cliffs, NJ, pp. 349–361.
- Bogaart, P.W., Van Balen, R.T., Kasse, C., Vandenbergh, J., 2003. Process-based modelling of fluvial system response to rapid climate change—I: model formulation and generic applications. *Quaternary Science Reviews* 22, 2077–2095.
- Boylan, A., Waltham, D.A., Bosence, D.W.J., Badenas, B., Aurell, M., 2002. Digital rocks: linking forward modelling to carbonate facies. *Basin Research* 14, 401–415.
- Braun, J., Sambridge, M., 1997. Modelling landscape evolution on geological time scales: a new method based on irregular spatial discretization. *Basin Research* 9, 27–52.
- Braun, J., Thieulot, C., Fullsack, P., DeKool, M., Beaumont, C., Huismans, R., 2008. DOUAR: a new three-dimensional creeping flow numerical model for the solution of geological problems. *Physics of the Earth and Planetary Interiors. Physics of the Earth and Planetary Interiors* 171, 76–91.
- Bull, W.B., 1977. The alluvial fan environment. *Progress in Physical Geography* 1, 222–270.
- Bull, W.B., 1991. *Geomorphic Responses to Climate Change*. Oxford University Press, New York. 326 pp.
- Bull, W.B., 1996. Global climate change and active tectonics: effective tools for teaching and research. *Geomorphology* 16, 217–232.
- Chen, C.L., 1986. Chinese concepts of modeling hyperconcentrated streamflow and debris flow. *Proceedings of the Third International Symposium on River Sedimentation*, Jackson, Mississippi, pp. 1647–1657.
- Clevis, Q., de Boer, P., Wachter, M., 2003. Numerical modelling of drainage basin evolution and three-dimensional alluvial fan stratigraphy. *Sedimentary Geology* 163, 85–110.
- Cowie, P.A., Attal, M., Tucker, G.E., Whittacker, A.C., Naylor, M., Gansas, A., Roberts, G.P., 2006. Investigating the surface process response to fault interaction and linkage using a numerical modelling approach. *Basin Research* 18, 231–266.
- Culling, W.E.H., 1960. Analytical theory of erosion. *Journal of Geology* 68, 336–344.
- De Chant, L.J., Pease, P.P., Tchakerian, V.P., 1999. Modelling alluvial fan morphology. *Earth Surface Processes and Landforms* 24, 641–652.
- Decker, K., Peresson, H., Hinsch, R., 2005. Active tectonics and Quaternary basin formation along the Vienna Basin transform fault. *Quaternary Science Reviews* 24, 305–320.
- Einsele, G., Hinderer, M., 1998. Quantifying denudation and sediment-accumulation systems (open and closed lakes): basic concepts and first results. *Palaeogeography, Palaeoclimatology, Palaeoecology* 140, 7–21.
- Faber, R., Wagreich, M., 2005. Modelling of topography and sedimentation along synsedimentary faults: WinGeol/SedTec. *Austrian Journal of Earth Sciences* 97, 60–66.
- Fink, J., 1955. Das Marchfeld, pp. 88–116. *Verh. Geol. B.-A., Spec. Vol. D*.
- Fink, J., Kukla, G., 1977. Pleistocene climates in central Europe. *Quaternary Research* 7, 363–371.
- Gordon, I., Heller, P.L., 1993. Evaluating major controls on basinal stratigraphy, Pine Valley, Nevada: implications for syntectonic deposition. *Geological Society of America Bulletin* 105, 47–55.
- Harvey, A.M., 2002a. Effective timescales of coupling within fluvial systems. *Geomorphology* 44, 175–201.
- Harvey, A.M., 2002b. The role of base-level change in the dissection of alluvial fans: case studies from southeast Spain and Nevada. *Geomorphology* 45, 67–87.
- Harvey, A.M., Silva, P.G., Mather, A.E., Goy, J.L., Stokes, M., Zazo, C., 1999. The impact of Quaternary sea-level and climatic change on coastal alluvial fans in the Cabo de Gata ranges, southeast Spain. *Geomorphology* 28, 1–22.
- Habersack, H., 2005. Schwebstoffmessungen an den Pegelstellen Mureck/Mur und Feldbach/Raab, Department für Wasser - Atmosphäre - Umwelt. Institut für Wasserwirtschaft, Hydrologie und konstruktiven Wasserbau, Vienna, Austria. University of Life Sciences.
- Havinga, 1972. A palynological investigation in the Pannonian climate region of Lower Austria. *Review of Palaeobotany and Palynology* 14, 319–352.
- Hinsch, R., Decker, K., Wagreich, M., 2005. 3-D mapping of segmented active faults in the southern Vienna Basin. *Quaternary Science Reviews* 24, 321–336.
- Hodel, H., Lehmann, C.h., 2000. Mittlere Fließgeschwindigkeiten in Wildbächen und Gebirgsflüssen – Welche Maximalwerte sind realistisch? *International Symposium Interpraevent 2000, Villach / Austria*.
- Högger, N., 1980. Repeated levelling and vertical crustal movements. Problems and results. *Rock Mechanics (Suppl. 9)*, 201–212.
- Krieger, I.M., Dougherty, T.J., 1959. A mechanism of non-Newtonian flow in suspension of rigid spheres. *Transactions of the Society of Rheology* 3, 137–152.
- Küpper, H., 1950. Zur Kenntnis des Alpenabbruchs am Westrand des Wiener Beckens. *Jb. Geol. B.A.*, 94.
- Leeder, M.R., Harris, T., Kirkby, M.J., 1998. Sediment supply and climate change: implications for basin stratigraphy. *Basin Research* 10 (1), 7–18.
- Molnar, P., England, P., 1990. Late Cenozoic uplift of mountain ranges and global cooling: chicken or egg? *Nature* 346, 29–34.
- Nemec, W., Postma, G., 1993. Quaternary alluvial fans in southwestern Crete; sedimentation processes and geomorphic evolution. In: Marzo, M., Puigdefabregas, C. (Eds.), *Alluvial Sedimentation: Int. Ass. Sedimentol., Spec. Publ.*, pp. 235–276.
- Oldfield, F., 2005. *Environmental Change*. Cambridge University Press, Cambridge.
- Paola, C., 2000. Quantitative models of sedimentary basin filling. *Sedimentology* 47, 121–178.
- Ritter, J.B., Miller, J.R., Enzel, Y., Wells, S.G., 1995. Reconciling the roles of tectonics and climate in Quaternary alluvial fan evolution. *Geology* 23, 245–248.
- Salcher, B., 2008. *Sedimentology and Modelling of the Mitterndorf Basin*, PhD Thesis. University of Vienna, Vienna: 107 pp.
- Salcher, B., Wagreich, M., in press. Climate and tectonic controls on sequence development and river evolution in Austria's largest Pleistocene basin. *Quaternary International*. doi:10.1016/j.quaint.2009.04.007.
- Schulze, K., Hunger, M., Döll, P., 2005. Simulating river flow velocity on global scale. *Advances in Geosciences* 133–136 2005.
- Shanley, K.W., McCabe, P.J., 1994. Perspectives on the sequence stratigraphy of continental strata. *American Association of Petroleum Geologists, Bulletin* 78, 544–568.
- Slingerland, R.S., Harbaugh, J.W., Furlong, K.P., 1994. *Simulating Clastic Sedimentary Basins*. Prentice-Hall, Englewood Cliffs, NJ. 220 pp.
- Stock, J.D., Montgomery, D.R., 1999. Geologic constraints on bedrock river incision using the streampower law. *Journal of Geophysical Research* 104, 4983–4993.
- Tucker, G., Slingerland, R.L., 1994. Erosional dynamics, flexural isostasy, and long-lived escarpments: a numerical modeling study. *Journal of Geophysical Research* 99 (B6), 12,229–12,243.
- Van Husen, D., 1987. *Die Ostalpen in den Eiszeiten*. Verlag der Geol. B.A., 24 pp.
- Van Husen, D., 2000. Geological processes during the Quaternary. *Mitteilungen der Österreichischen Geologischen Gesellschaft* 92, 135–156.
- Vandenbergh, J., 2002. The relation between climate and river processes, landforms and deposits during the Quaternary. *Quaternary International* 91, 17–23.
- Vandenbergh, J., 2008. The fluvial cycle at cold–warm–cold transitions in lowland regions, a refinement of theory. *Geomorphology* 98, 275–284.
- Viseras, C., Calvache, M.L., Soria, J.M., Fernández, J., 2003. Differential features of alluvial fans controlled by tectonic or eustatic accommodation space. Examples from the Betic Cordillera, Spain. *Geomorphology* 50, 181–202.
- Waltham, D., Jaffey, N., MacLean, S., Zampetti, V., 2008. Stratigraphic modelling of turbidite prospects to reduce exploration risk. *Petroleum Geoscience* 14, 273–280.
- Warrlich, G., Bosence, D., Waltham, D., Wood, C., Boylan, A., Badenas, B., 2008. 3D stratigraphic forward modelling for analysis and prediction of carbonate platform stratigraphies in exploration and production. *Marine and Petroleum Geology* 25, 25–58.
- Weissmann, G.S., Mount, J.F., Fogg, G.E., 2002. Glacially driven cycles in accumulation space and sequence stratigraphy of a stream-dominated alluvial fan, San Joaquin Valley, California, U.S.A. *Journal of Sedimentary Research* 72, 240–251.
- Weissmann, G.S., Bennett, G.L., Lansdale, A.L., 2005. Factors controlling sequence development on Quaternary fluvial fans, San Joaquin Basin, California, USA. *London Special Publication* 251, 169–186.
- Wells, S.G., Harvey, A.M., 1987. Sedimentologic and geomorphic variations in storm-generated alluvial fans, Howgill Fells, northwest England. *Geological Society of America, Bulletin* 98, 182–198.
- Whipple, K.H., Trayler, C.R., 1996. Tectonic control of fan size: the importance of spatially variable subsidence rates. *Basin Research* 8, 351–366.
- Willgoose, G., Bras, R.L., Rodriguez-Irtube, I., 1991. Results from a model river basin evolution. *Earth Surface Processes and Landforms* 16, 237–254.
- Willis, K.J., Rudner, E., Sümege, P., 2000. The full-glacial forests of central and southeastern Europe. *Quaternary Research* 53, 203–213.
- Wu, J.E., McClay, K., Whitehouse, P., Dooley, T., 2009. 4D analogue modelling of transtensional pull apart basins. *Marine and Petroleum Geology* 26, 1608–1623.